Proceedings of Symposium on Ultrasonic Electronics, Vol. 35 (2014) pp. 557-558
3-5 December, 2014

3-Dimensional Convergence Properties of Off-Axis Aplanatic Straubel Acoustic Mirror

軸外しアプラナート・シュトラウベル音響反射鏡の 3 次元集束特性

Yuji Sato[1], Yuki Usami[2], Hanako Ogasawara[2], Koichi Mizutani[1] and Toshiaki Nakamura[2] ([1] Univ. of Tsukuba; [2] National Defense Academy)
佐藤裕治[1]，宇佐美勇輝[2]，小笠原英子[2]，水谷孝一[1]，中村敏明[2] ([1]筑波大院，[2]防衛大)

1. Introduction

Underwater acoustic imaging technology is effective for marine resource detection, coastal security, and maintenance of seashore facilities. Underwater acoustic lenses and acoustic mirrors made an effort on reducing sound attenuation, aberration, and having stability for water temperature change[1-3]. In the past study, we designed an aplanatic Straubel (AS) mirror[4]. The AS mirror is an aplanatic back-surface mirror. The AS mirror could correct spherical and coma aberrations in the result of experiment[5]. However, the AS mirror has a problem. The receiver array is located in front of the mirror, which results in the interruption of incident sound waves, and then we designed an off-axis AS mirror and evaluated the convergence properties by numerical calculations[6].

In this study, we calculate the convergence properties of an off-axis AS mirror as shown in Fig. 1 for two incident waves with different directions around *x*-axis and *y*-axis as shown in Fig. 2.

2. Evaluation by numerical calculation

2.1 Calculation method

In this subsection, aberration and attenuation using a numerical calculation based on the wave theory are considered and the convergence property is evaluated in terms of the beam width, which determines the resolution of the acoustic images. The details of the three-dimensional calculation method are described in ref. 3. The surfaces of silicone rubber and the rigid body are discretized into about 30,000 quadrangle elements. A point source is assumed to be located at (-100tanθ_x, -100 tanθ_y, 100) (m). Here, θ_x is the incident angle from the *z*-axis toward the *x*-direction. The point source transmits a sinusoidal wave of 500 kHz. The particle velocity on a discretized surface of silicone rubber is calculated using the Rayleigh integral. The virtual secondary point sources, which produce particle velocity identical to the normal component of the calculated particle velocities, are regarded to be distributed on the surface of silicone rubber. Then, the particle velocities on the surfaces of the rigid body and silicone rubber are calculated in sequence. The amplitudes of sound fields focused by the different mirrors cannot be compared in this calculation method because the surfaces are regarded as source arrays. However, it is possible to calculate the distributions such as that of beam widths and verify the aberration effect corresponding to each incident angle. Multiple reflections and diffractions from the outside of a mirror are omitted in the calculation. The sound speed, density, and attenuation coefficient for the lens made of silicone rubber and water are shown in Table 1.

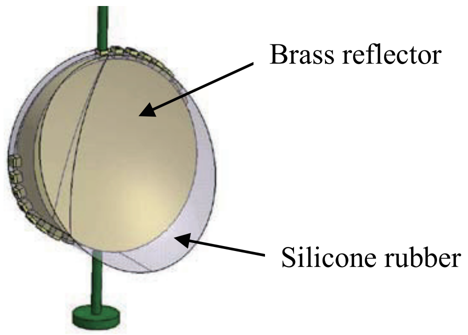

Fig. 1 Off-axis aplanatic Straubel acoustic mirror made of silicone rubber and brass with the diameter of 200 mm.

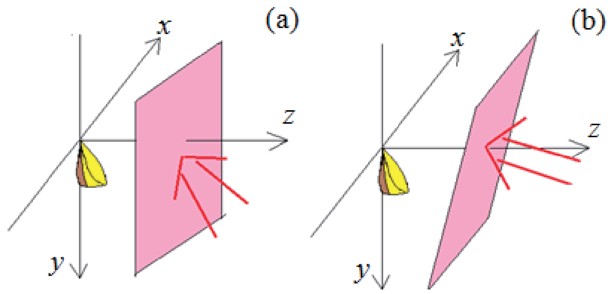

Fig. 2 Coordinate systems of off-axis AS mirror for two incident directions around *x*-axis and *y*-axis.
The colored rectangular areas show examples of incident wave fronts with (a) θ_x = -15°, θ_y = 0° and (b) θ_x = 0°, θ_y =15°.

yuji@aclab.esys.tsukuba.ac.jp

Table 1 Parameters used in the calculation.

	Water	Silicone rubber
Sound speed (m/s)	1500	1000
Density (kg/m^3)	1000	1490
Attenuation coefficient (Np/m)	0	57.6

Figures 2(a) and 2(b) show the direction of the incident wave for the off-axis AS mirror. In Fig. 2(a), incident wave front is parallel to the *y*-axis but has the angle of -15° to the *x*-axis. In Fig. 2(b), incident wave front is parallel to the *x*-axis but has the angle of 15° to the *y*-axis.

2.2 Calculation results

The calculated sound power distributions of -3 dB area around focus on *y-z* plain at *x*=0 are shown in Fig. 3 for the incidence direction from θ_x = -15° to 15° at 5° step as shown in Fig. 2(a). This figure shows a section sliced at *y*=0. We need calculate a 3-dimensional structure of the convergence field of the AS mirror according to various sliced section with different *y*- coordinate.

Then the sound power distributions of -3 dB area around focus on *y-z* plain at *x*=0 are shown in Fig. 4

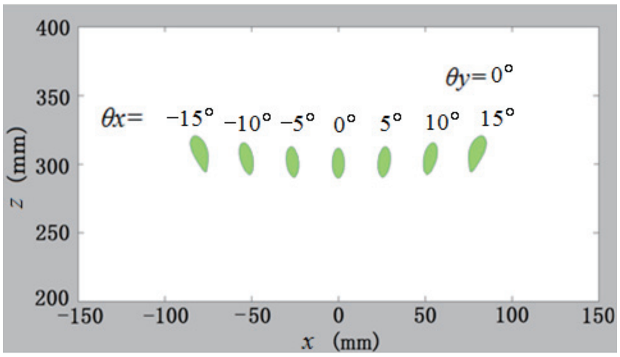

Fig. 3 Sound power distributions of -3 dB area around focus on *x-z* plain at *y*=0 focused by off-axis AS mirror.

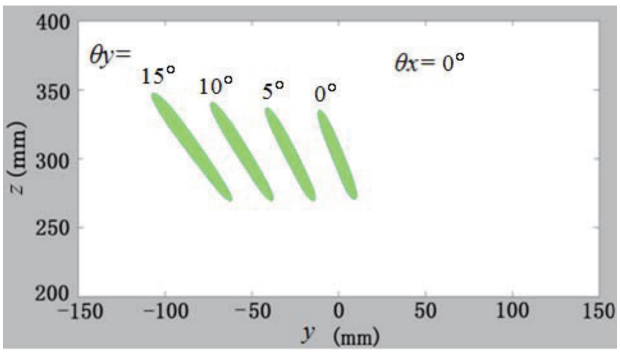

Fig. 4 Sound power distributions of -3 dB area around focus on *y-z* plain at *x*=0 focused by off-axis AS mirror.

for the incidence direction from θ_y = 0° to 15° at 5° step as shown in Fig. 2(b). These data show sections sliced at *x*=0, and are similar patterns to our preliminary experimental results[7, 8]. We need verify these patterns for wider incident angle by the experiments in water tank.

3. Conclusion

An incident sound wave coming into an ordinary AS mirror is interrupted by a receiver array. Thus, an off-axis AS mirror was proposed to solve this problem. We evaluated the convergence properties of the off-axis AS mirror for two incident planes by the numerical method

From the results of the calculation, the convergence properties on two sections of the off-axis AS mirror were obtained from θ_y = 0° to 15° incidence on the *y-z* plain at *x*=0, and from θ_x = -15° to 15° incidence on the *x-z* plain at *y*=0.

We will evaluate the 3-dimensional convergence properties by calculating of many sliced sections, and compare with the experimental data of the 3-dimensional convergence properties obtained by rotating the mirror around *z*-axis in water tank in near future.

Acknowledgment

This work was partly supported by a Grant-in-Aid for Scientific Research by Japan Society for the Promotion of Science (24560998).

References

1. S. Yoshida: Research Institute for Scientic Measurements Tohoku University, **6** (1958) 122 [in Japanese].
2. Y. Sato, A. Miyazaki, K. Mori, and T. Nakamura: Jpn.J. Appl. Phys., **46** (2007) 1987.
3. Y. Sato, K. Mizutani, N. Wakatsuki, and T. Nakamura: Jpn. J. Appl. Phys. **49** (2010) 07HG03.
4. Y. Sato, K. Mizutani, N. Wakatsuki, and T. Nakamura: Jpn. J. Appl. Phys. **50** (2011) 07HG08.
5. S. Nishimoto, Y. Sato, K. Mizutani, N. Wakatsuki, and T. Nakamura: Proc. of Ultrasonic Electronics 2011, (2011) 431.
6. Y. Sato, K. Mizutani, N. Wakatsuki, and T. Nakamura: Jpn. J. Appl. Phys. **51** (2012) 07GG12-1.
7. Y, Sato, H. Sato, H. Ogasawara, K. Mizutani, and T. Nakamura: Proc. of Ultrasonic Electronics 2013, (2013) 363.
8. Y, Sato, H. Ogasawara, K. Mizutani, and T. Nakamura: Proc. of Underwater Acoustics 2014, (2014) 1633.